Received: 15 April 2024 | Revised: 27 June 2024 | Accepted: 8 July 2024
DOI: 10.1002/app.56045

RESEARCH ARTICLE

Applied Polymer SCIENCE WILEY

Effect of partial replacement of antimony trioxide with zinc borate and stannic oxide on the flame retardancy of flexible PVC films

Yongsen Zhang[1,2,3] | Lijun Qian[1,2,3] | Lijie Qu[1,2,3] | Jingyu Wang[1,2,3] | Yong Qiu[1,2,3] | Wang Xi[1,2,3] | Yao Ma[4]

[1]School of Light Industry Science and Engineering, Beijing Technology and Business University, Beijing, China

[2]China Light Industry Engineering Technology Research Center of Advanced Flame Retardants, Beijing, China

[3]Petroleum and Chemical Industry Engineering Laboratory of Non-halogen Flame Retardants for Polymers, Beijing, China

[4]Benecke-Changshun Auto Trim (Zhangjiagang) Co. Ltd, Zhangjiagang, China

Correspondence
Lijun Qian and Lijie Qu, School of Light Industry Science and Engineering, Beijing Technology and Business University, Beijing, 100048, China.
Email: qianlj@btbu.edu.cn and qulijie@btbu.edu.cn

Funding information
National Natural Science Foundation of China, Grant/Award Numbers: 12302272, 22005009, 52203055; Natural Science Foundation of Beijing Municipality, Grant/Award Number: 2222052; R&D Program of Beijing Municipal Education Commission, Grant/Award Number: KM202210011004

Abstract

Replacing antimony trioxide (Sb_2O_3) with an environmentally friendly alternative is of great scientific and commercial value for studying the flame retardant properties of flexible PVC (fPVC) films in automotive interior materials. This study develops flame retardant fPVC films with reduced Sb_2O_3 content by introducing stannic oxide (SnO_2) and zinc borate (ZB). The results indicate that the fPVC film with ZB partially replacing Sb_2O_3 exhibits superior flame retardancy and smoke suppression compared to the product containing SnO_2. The peak heat release rate (PHRR), total heat release (THR), and total smoke release (TSR) of 2ZB/2Sb_2O_3 fPVC film are reduced by 32.1%, 27.5%, and 22.1%, respectively, compared to that of 4Sb_2O_3 contained fPVC film. The increase in flame retardancy is attributed to the presence of ZB, which compensates for the deficiency of char formation ability of Sb_2O_3 in the condensed phase. The PHRR and THR of 2SnO_2/2Sb_2O_3 fPVC film decrease by 27% and 12.5%, respectively, compared to that of 4Sb_2O_3 fPVC film, while the TSR increases by 16.5%. This study develops a straightforward approach to creating a flame retardant fPVC film that is suitable for the latest industrial application in automotive interior materials.

KEYWORDS

films, flame retardance, functionalization of polymers, thermal properties

1 | INTRODUCTION

In recent years, the rapid development of electrical vehicles has brought about serious fire safety concerns,[1] especially on the automobile interior materials occupied a significant amount of space inside the car. In the event of a fire, it can cause significant harm to the health and property of passengers and drivers.[2] Therefore, the development of flame retardant automotive interior materials has become a hot research topic in recent years.[3,4] Flexible PVC (fPVC, PVC powder: plasticizer = 50:50) films are known for their notable characteristics, including wear resistance, aging resistance, flexibility, soft texture, and cost-effectiveness.[5] fPVC films are widely utilized as automotive interior materials, such as seat backs, seat cushions, dashboards, door panels,

headrests, and center consoles. As a substantial amount of the interior space in automobiles is made up of them, the fire safety of fPVC film is of utmost importance.[6]

Diantimony trioxide (Sb_2O_3), as a previously commonly used flame retardant for fPVC films,[7,8] present outstanding flame retardant efficiency in halogenated polymers due to the synergistic effect of the antimony-halogen system.[9] However, it has been demonstrated that Sb_2O_3 can produce toxic fumes derived from Sb compounds under combustion conditions,[10,11] which has a detrimental impact on human health and the environment.[12–14] As a result, it has been listed as carcinogens and restricted substances according to the World Health Organization's, International Agency, and RoHS of the European Union. Therefore, the development of environmentally friendly and efficient flame retardants to replace the harmful Sb_2O_3 has become a popular research topic for fPVC films due to concerns for environmental friendliness and human health.[15–17]

Synergistic blending was a crucial method for significantly improving the flame retardancy of materials.[18] Previous studies have demonstrated that Sn has a positive synergistic flame retardant effect with fPVC films.[19,20] Of the Sn-containing flame retardants, stannic oxide (SnO_2) improved the flame retardancy of fPVC films while maintaining their excellent mechanical properties.[21] Additionally, SnO_2 is an environmentally friendly flame retardant with better safety.[22] Zinc borate (ZB, 2.85 \$ kg^{-1}) was a halogen-free flame retardant that was more cost-effective than SnO_2 (37.65 \$ kg^{-1}).[23,24] Furthermore, ZB exhibits favorable thermal stability and smoke suppression characteristics. The decomposition of ZB produced zinc oxide (ZnO) and boron trioxide (B_2O_3), both of which promoted the production of more char layer in the matrix. These char layer played a role in isolating the air and reducing the exchange of heat, which enhanced the condensed phase flame retardant effect of the materials. When used as a replacement for Sb_2O_3 (11.25 \$ kg^{-1}), ZB improved the flame retardancy and smoke suppression properties of the material while significantly reducing its cost.[25,26]

Therefore, this work chose SnO_2 and ZB to replace Sb_2O_3 to prepare flame retardant fPVC films. The flame retardant and mechanical properties of the fPVC films were studied extensively. The corresponding conclusion possessed significant scientific and practical value for the development of a new generation of environmentally friendly, cost-effective, safe, and flame retardant automotive interior materials.

2 | EXPERIMENTAL

2.1 | Raw materials

PVC powder (BPR-1069) was acquired from Jiangsu Kangning Chemical Co., Ltd. The plasticizer (DPHP) was purchased from UPC Technology Corporation, and the stabilizer (T8003) was gained by Changzhou Youjia New Material Technology Co., Ltd. Furthermore, the foam agent (ST-13) was obtained from Zhejiang Shuntai Rubber and Plastic Technology Co., Ltd. Jiangsu Standard and Prosperity Additives Co., Ltd provided Sb_2O_3 (TD8250, 99.8%). Nangong City Yingtai Metal Materials Co., Ltd provided SnO_2 (Grade, 99.9%), and ZB (LD-202, 99.8%) was provided by Henan Jijia Chemical Products Co., Ltd.

2.2 | Sample preparation

The fPVC slurry was prepared by mixing PVC powder, plasticizer, stabilizer, foam agent, and flame retardants in a vacuum mixer (MD003-7-type equipment, Zhangjiagang Hongtai Industrial Equipment Manufacturing Co., Ltd.) and stirring at a speed of 1500 rpm for 10 min. The detailed formulation was displayed in Table 1.

The fPVC slurry was subsequently coated and dried in a Martin oven (LAB032-4-type equipment, Mathis company, Switzerland) at a temperature of 200°C for 90 s, yielding fPVC films with a thickness of 0.3 mm.

2.3 | Characterization

The limiting oxygen index (LOI) test was conducted using the 300,800-type equipment manufactured by Concept Instrument Co., Ltd. of the UK in strict accordance with the GB/T 2406.2-2009 standard. The sample size was 140 mm × 52 mm × 0.3 mm. Each set of data was obtained by testing at least five samples.

The FTT0082-type vertical/horizontal burning test box, produced by fire testing technology (FTT), was used to perform the horizontal burning test in accordance with the GB 8410-2006 standard. The sample size was 356 mm × 100 mm × 0.3 mm. Each set of data was tested with at least five samples.

The cone calorimeter test (CCT) was conducted using the FTT0007-type equipment, also produced by FTT, following the ISO 5660-1 standard. The fPVC film was tested with a sample size of 100 mm × 100 mm × 0.3 mm and an irradiation power of 50 $kW \cdot m^{-2}$. At least two samples were tested for each data.

TABLE 1 Formulation of flexible PVC (fPVC) films.

Sample	PVC powder/phr	Plasticizer/phr	Stabilizer/phr	Foam agent/phr	SnO_2/phr	ZB/phr	Sb_2O_3/phr
fPVC	50	50	1	1	0	0	0
$4Sb_2O_3$	50	50	1	1	0	0	4
$1SnO_2/3Sb_2O_3$	50	50	1	1	1	0	3
$2SnO_2/2Sb_2O_3$	50	50	1	1	2	0	2
$3SnO_2/1Sb_2O_3$	50	50	1	1	3	0	1
$4SnO_2$	50	50	1	1	4	0	0
$1ZB/3Sb_2O_3$	50	50	1	1	0	1	3
$2ZB/2Sb_2O_3$	50	50	1	1	0	2	2
$3ZB/1Sb_2O_3$	50	50	1	1	0	3	1
4ZB	50	50	1	1	0	4	0

Thermogravimetric analyzer and Fourier transform infrared spectrometer (TG-FTIR) was tested using the STA 8000-type equipment for analyzing the thermal decomposition products of materials and monitoring the release of volatile compounds in real time. The sample, placed in an alumina crucible with a mass of 10 ± 0.1 mg, was heated from 50 to 600°C at a rate of 20°C·min^{-1} under N_2 atmosphere. The temperature of the FTIR sample chamber and transfer line was maintained at 280°C.

The microstructures and element content were analyzed using the Phenom-World Pro X analyzer with scanning electron microscope-energy dispersive spectrometer (SEM-EDS). The purpose of this experiment was to observe the residual char morphology and element retention of fPVC films after the horizontal burning test. The operating voltage was 10 kV.

The tensile test was conducted using the BT2-FR005TE-type universal material testing machine from ZwickRoell in Germany, following the ISO 527-1 standard. The sample size was 250 mm × 20 mm × 0.3 mm. Each set of data was gathered from testing a minimum of five samples.

3 | RESULTS AND DISCUSSION

3.1 | Flame resistance and self-extinguishing performance

The flame resistance and self-extinguishing performance of fPVC films were evaluated through LOI and horizontal burning test. The results of the horizontal burning and the real-time trace for fPVC films were presented in Figure 1. The specific data for the LOI test and horizontal burning test were listed in Table 2.

Partial substitution of Sb_2O_3 with SnO_2 increased the LOI of fPVC films from 23.2% ($4Sb_2O_3$ fPVC film) to 23.6%, while partial replacement with ZB increased the LOI up to 23.8%. The data indicated a possible synergistic flame retardant effect between SnO_2/Sb_2O_3 and ZB/Sb_2O_3. In addition, partial substitution of Sb_2O_3 further improved the flame retardancy of fPVC films.[27,28]

The rate of flame propagation in automotive interior materials can be accurately measured by the horizontal burning test.[29] The reduction of the rate of flame propagation in a material can provide more time for individuals who have become trapped in a fire to escape.[30] Figure 1 showed a real-time trace of the ignition and burn stage of the fPVC films in horizontal burning test. The pure fPVC film burned beyond the first mark before the ignition time ended and continued to burn until it passed the second mark, resulting in a horizontal burning rating of E, and the horizontal burning rate was exceptionally high at 354.4 ± 16.7 mm·min^{-1}, indicating a severe fire hazard. The fPVC film containing $4Sb_2O_3$ achieved a horizontal combustion rating of A, and the flame was extinguished before reaching the first mark. This was due to the halogen-antimony synergistic flame retardant effect between Sb_2O_3 and fPVC.[9] The fPVC film containing $2SnO_2/2Sb_2O_3$ and $2ZB/2Sb_2O_3$ both have a horizontal burning rating of A. Surprisingly, the flame damage length of the materials was shorter and the flame observably extinguished during ignition compared to the $4Sb_2O_3$ fPVC film, which represented a further enhancement in flame retardancy. The horizontal burning rate of fPVC films containing $4SnO_2$ and 4ZB were 287.5 ± 22.3 mm·min^{-1} and 310.7 ± 10.2 mm·min^{-1}, respectively, resulting in a horizontal burning rating of E. The above results confirmed the synergistic flame retardancy between SnO_2/Sb_2O_3 and ZB/Sb_2O_3.

In summary, these results indicated that the combination of SnO_2/Sb_2O_3 and ZB/Sb_2O_3 has a considerable effect on decreasing the horizontal burning rate of the fPVC films. This was due to the ability of SnO_2 or ZB to promote early cross-linking and the formation of more

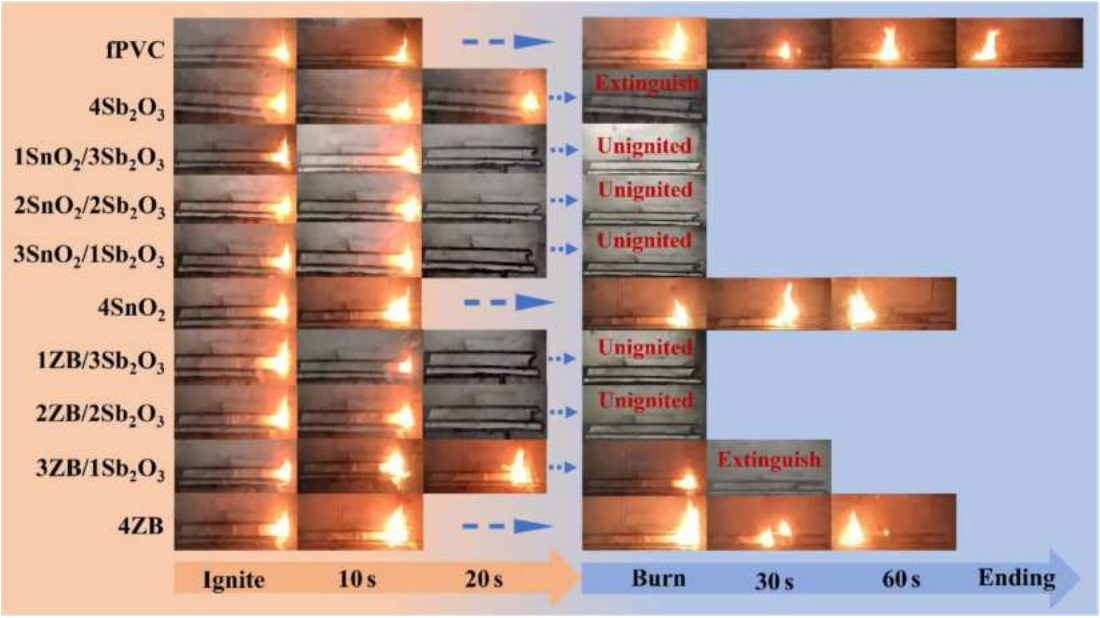

FIGURE 1 Results of the horizontal burning rate and real-time trace for flexible PVC (fPVC) films. [Color figure can be viewed at wileyonlinelibrary.com]

TABLE 2 Limiting oxygen index (LOI) and horizontal burning test data of flexible PVC (fPVC) films.

Sample	LOI (%)	Horizontal burning test		
		V (mm·min^{-1})[a]	Dripping	Rating[b]
fPVC	19.0	354.4 ± 16.7	Yes	E
$4Sb_2O_3$	23.2	0	No	A
$1SnO_2/3Sb_2O_3$	23.5	0	No	A
$2SnO_2/2Sb_2O_3$	23.6	0	No	A
$3SnO_2/1Sb_2O_3$	23.1	0	No	A
$4SnO_2$	22.0	287.5 ± 22.3	No	E
$1ZB/3Sb_2O_3$	23.8	0	No	A
$2ZB/2Sb_2O_3$	23.6	0	No	A
$3ZB/1Sb_2O_3$	21.5	162.0 ± 6.7	No	B
4ZB	19.6	310.7 ± 10.2	Yes	E

[a]The horizontal burning rate: $V = 60 \times Ld/Tb$, where L_d, the length of damage after the flame has burned through the first marker, T_b, the time from the moment the flame passed through the first marker until it was extinguished or passed through the second marker.
[b]The horizontal burning rating, in descending order, was as follows: A (The flame extinguished before it reached the first marker), B (The flame self-extinguished within 60 s and burned no more than 50 mm away), C (The flame past the first marker but not past the second), D (The flame burned past the second marker), and E (No rating, the flame burned to the first marker in the ignition process).

residual char in the matrix of the fPVC films,[31,32] which enabled the fPVC films to self-extinguish rapidly.

3.2 | Analysis of combustion behavior

The CCT can simulate the heat release and smoke generation of materials in a real fire environment,[33,34] and provide a valuable reference for evaluating the combustion behavior of materials in real fires.[35,36] Figure 2 and Table 3 presented the specific data of the CCT.

Figure 2a showed the heat release rate (HRR) curve of fPVC films. The peak heat release rate (PHRR) of the $2SnO_2/2Sb_2O_3$ fPVC film was 230 kW·m^{-2}, which was 27% lower than that of the $4Sb_2O_3$ fPVC film. The replacement of 50% Sb_2O_3 by ZB reduced the PHRR of

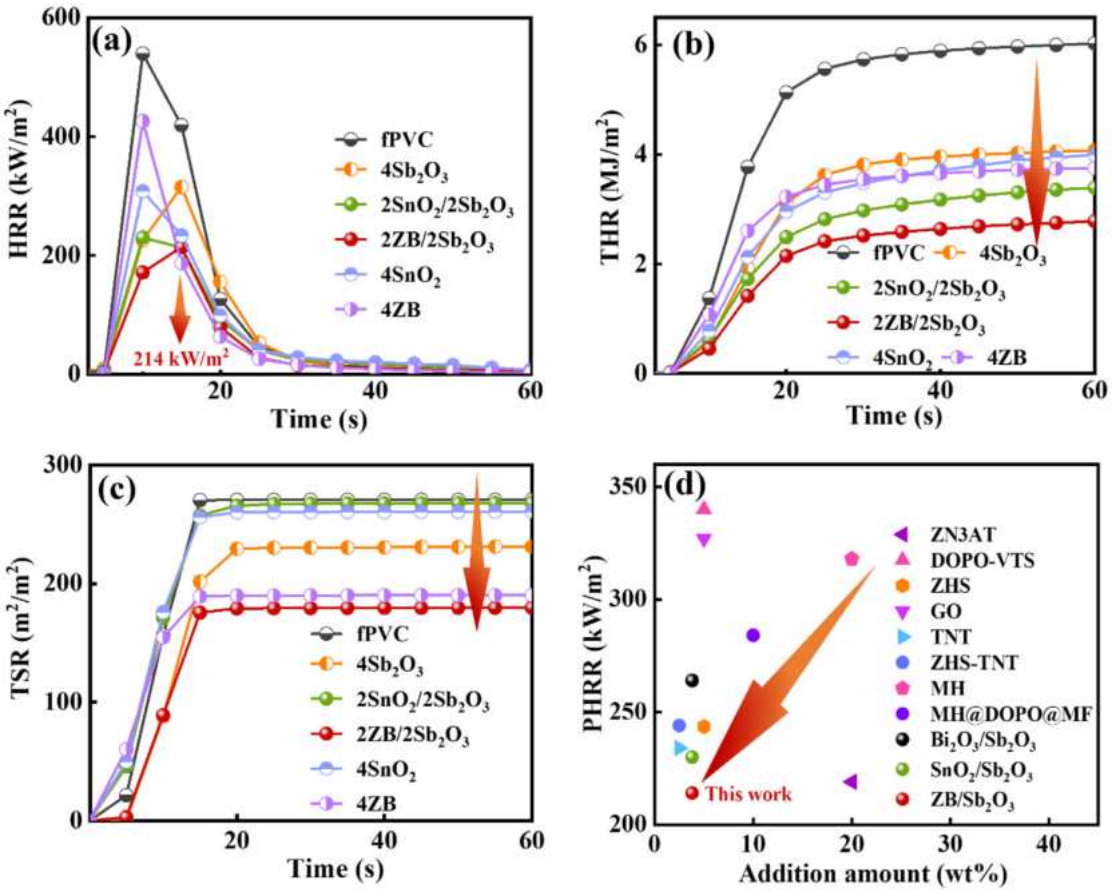

FIGURE 2 Cone calorimeter test (CCT) results of flexible PVC (fPVC) films (a) heat release rate (HRR), (b) total heat release (THR), (c) total smoke release (TSR), (d) some typical flame retardancy of fPVC films: ZN3AT,[42] DOPO-VTS,[43] ZHS,[43] GO,[44] TNT,[45] ZHS-TNT,[45] MH,[46] MH@DOPO@MF,[46] Bi_2O_3/Sb_2O_3,[47] SnO_2/Sb_2O_3 and ZB/Sb_2O_3). [Color figure can be viewed at wileyonlinelibrary.com]

TABLE 3 Cone calorimeter test (CCT) data of flexible PVC (fPVC) films.

Sample	TTF/s	PHRR/(kW·m^{-2})	THR/(MJ·m^{-2})	Av-EHC/(MJ·kg^{-1})	TSR/(m^2·m^{-2})
fPVC	12	539	5.8	19.8	271
$4Sb_2O_3$	23	315	4.0	13.0	231
$2SnO_2/2Sb_2O_3$	23	230	3.5	17.1	269
$2ZB/2Sb_2O_3$/(MJ/m^2)	16	214	2.9	12.8	180
$4SnO_2$	18	308	4.1	17.1	261
4ZB/(kg/kg)	17	426	3.7	15.8	190

the fPVC film to 214 kW·m^{-2}, which was 32.1% lower than that of the $4Sb_2O_3$ fPVC film. Additionally, the time to flame out (TTF) of the $2ZB/2Sb_2O_3$ fPVC film (16 s) was shorter than that of the $2SnO_2/2Sb_2O_3$ fPVC film (23 s). This results indicated that the incorporation of ZB not only reduced the burning intensity of the fPVC film, but also expedited the extinguishing of the flame.[37,38]

Figure 2b showed the total heat release (THR) curve of fPVC films. The THR of the $2SnO_2/2Sb_2O_3$ fPVC film was 3.5 MJ·m^{-2}, a 12.5% decrease compared to that of the $4Sb_2O_3$ fPVC film. The THR of the $2ZB/2Sb_2O_3$ fPVC film was further reduced to 2.9 MJ·m^{-2}, a 27.5% decrease compared to that of the $4Sb_2O_3$ fPVC film. The results indicated that replacing 50% of Sb_2O_3 with ZB reduced the THR of fPVC film more significantly compared to that of SnO_2. This reduction in THR further decreased the risk of fire and increased the chances of escape for both the drivers and passengers.

The average effective heat of combustion (av-EHC) is the average heat released by the combustion of the

combustible components of the volatiles formed by the thermal decomposition of the material,[39,40] and it measures the amount of heat released during the combustion of combustible gases.[41] The av-EHC of the $2SnO_2/2Sb_2O_3$ fPVC film was 17.1 $MJ \cdot kg^{-1}$, which was 24% higher than that of $4Sb_2O_3$ fPVC film. However, the av-EHC of the $2ZB/2Sb_2O_3$ fPVC film was lower than that of the $4Sb_2O_3$ fPVC film. This indicated that the introduction of ZB reduced the combustible gases in the gas phase compared to SnO_2. These results can be attributed to the fact that the decomposition of ZB produced refractory gases, which improved the gas phase flame retardancy of the material. Additionally, the charring effect of ZB in the condensed phase resulted in more fuels being retained in the fPVC matrix.[38]

Figure 2c showed the total smoke release (TSR) curve of fPVC films. The TSR of the $2SnO_2/2Sb_2O_3$ fPVC film was 269 $m^2 \cdot m^{-2}$, which increased by 16.5% compared to the $4Sb_2O_3$ fPVC film. This indicated that partial replacement Sb_2O_3 with SnO_2 cannot enhance the smoke suppression performance of fPVC films. However, the TSR of the $2ZB/2Sb_2O_3$ fPVC film was 180 $m^2 \cdot m^{-2}$, a 22.1% decrease compared to that of the $4Sb_2O_3$ fPVC film. This data indicated that the introduction of ZB reduced the concentration of smoke released during the combustion of fPVC films. The reduction in smoke emission can be attributed to the decomposition of ZB into ZnO and B_2O_3.[23] The ZnO effectively inhibited smoke emission, while B_2O_3 accelerated material dehydration and charring,[24] resulting in a more stable char layer that locked in more combustibles in the condensed phase.[28] This reduced the release of smoke fragments in the gas phase.[38]

Figure 2d showed the typical flame retardancy of fPVC films, including ZN3AT,[42] DOPO-VTS,[43] ZHS,[43] GO,[44] TNT,[45] ZHS-TNT,[45] MH,[46] MH@DOPO@MF,[46] Bi_2O_3/Sb_2O_3[47] in our previous jobs, SnO_2/Sb_2O_3 and ZB/Sb_2O_3. Among these flame retardant systems, the ZB/Sb_2O_3 system demonstrated the best flame retardant properties with low additions. Although all three flame retardant systems (Bi_2O_3/Sb_2O_3, SnO_2/Sb_2O_3, and ZB/Sb_2O_3) have the same additive amount in fPVC films, the ZB/Sb_2O_3 system achieved the lowest PHRR. This indicated that the ZB/Sb_2O_3 system can effectively decrease the burning intensity of fPVC films. Therefore, it has the potential to be used as a flame retardant system for automotive interior materials.

3.3 | Analysis of condensed phase charring behavior

To investigate the effects of SnO_2/Sb_2O_3 and ZB/Sb_2O_3 on the charring behaviors of the fPVC film, SEM-EDS was used to analyze the microscopic morphology, and elemental distribution of the residual char after the horizontal burning test, which was shown in Figure 3.

The elemental scan revealed the absence of Sb in the residual char of the $4Sb_2O_3$ fPVC film, indicating complete decomposition of Sb_2O_3 during the combustion process. Subsequently, Sb_2O_3 reacted with the HCl released from the fPVC film to form $SbCl_3$ gas,[9] which were released into the gas phase to isolate the oxygen, thereby producing a gas phase flame retardancy.[48]

The residual char of the fPVC film of $2SnO_2/2Sb_2O_3$, and $4SnO_2$, as well as $2ZB/2Sb_2O_3$, and 4ZB, contained white flame retardant particles, as shown in the electron micrographs. Elemental scans further demonstrated that these flame retardants retained in the condensed phase contained the Sn,[31] Zn,[38] and B,[39] and the presence of these elements enhanced the condensed phase flame retardancy of fPVC films.[23] Furthermore, the elemental scanning results showed that the residual char in the $2ZB/2Sb_2O_3$ fPVC film and 4ZB fPVC film contained a significant amount of O. This element was primarily concentrated and enriched in the ZB particles. It was assumed that this O element originated from ZnO and B_2O_3 resulting from the decomposition of ZB.[38,39] These compounds were retained in the condensed phase, which accelerated the cross-linking, and charring of the fPVC films, forming a more stable char layer.[28]

Moreover, the Cl elemental content in the residual char of $2SnO_2/2Sb_2O_3$ fPVC film and $2ZB/2Sb_2O_3$ fPVC film decreased from 13.93 wt% to 5.13 wt% and 7.19 wt%, respectively, compared to that of $4Sb_2O_3$ fPVC film. The above results can be explained by the following hypothesis. At the beginning of the de—HCl process, SnO_2 or ZnO trapped some of the HCl,[24,31] producing a strong Lewis acid ($SnCl_2$ or $ZnCl_2$).[28,38] These Lewis acid catalyzed the decomposition of the fPVC film, promoting early cross-linking[37] and generating more residual char,[23] which exhibited condensed phase flame retardancy during combustion process.

3.4 | Thermal performance analysis

To investigate the effects of SnO_2/Sb_2O_3 and ZB/Sb_2O_3 on the thermal stability of fPVC films, the thermal decomposition behavior and char formation properties of fPVC films were analyzed by thermogravimetric analysis (TGA) and derivative thermogravimetry (DTG). Table 4 listed some characteristic thermogravimetric data of the fPVC films, and Figure 4 showed the TGA and DTG curves of the fPVC films.

Between 227 and 370°C, the mass loss was primarily due to the degradation of plasticizer and the removal of HCl from the fPVC film to form conjugated double

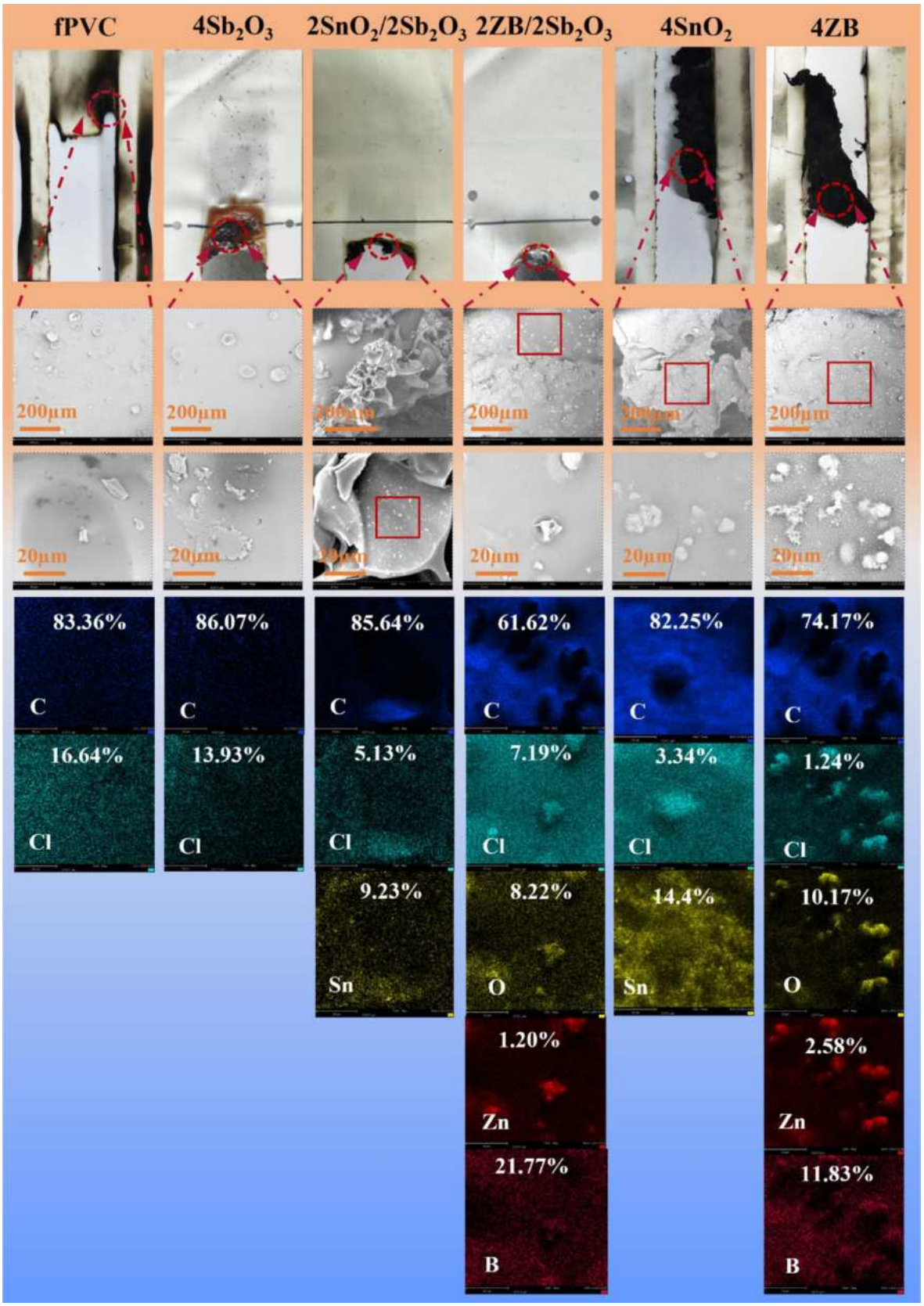

FIGURE 3 Scanning electron microscope-energy dispersive spectrometer (SEM-EDS) of the residual char after horizontal burning test of flexible PVC (fPVC) films. [Color figure can be viewed at wileyonlinelibrary.com]

TABLE 4 TGA test data of flexible PVC (fPVC) films.

Sample	$T_{5\%}$ (°C)	T_{max1} (°C)	T_{max2} (°C)	R_{600} (wt%)
fPVC	266.2	314.7	451.1	5.2
$4Sb_2O_3$	266.8	328.9	454.1	5.6
$2SnO_2/2Sb_2O_3$	248.4	292.0	471.3	11.2
$2ZB/2Sb_2O_3$	260.7	262.1	468.4	14.8
$4SnO_2$	250.0	261.5	473.2	14.9
4ZB	234.0	262.5	472.4	18.1

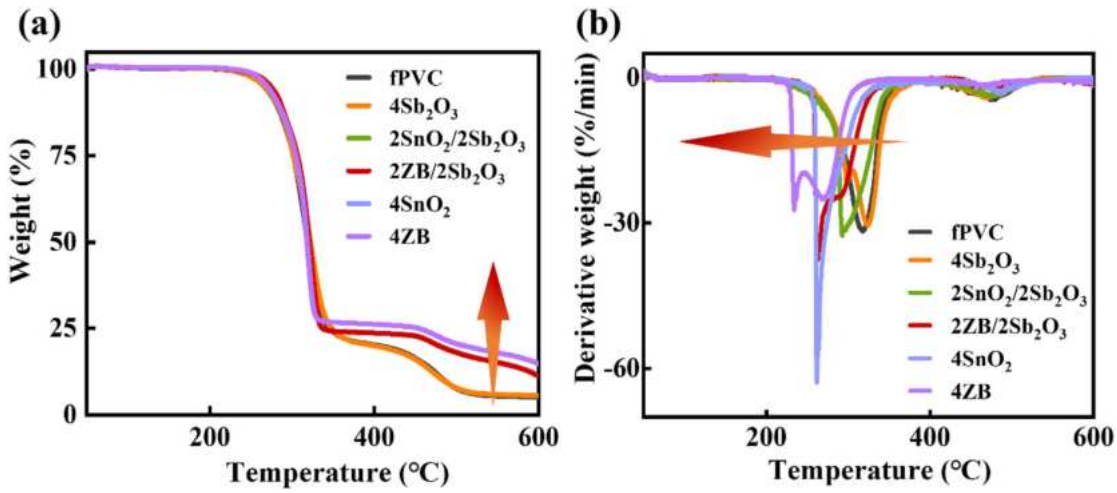

FIGURE 4 TGA and DTG curves of flexible PVC (fPVC) films ((a) TGA, (b) DTG). [Color figure can be viewed at wileyonlinelibrary.com]

bonds.[49] The initial decomposition temperature ($T_{5\%}$) of the $2SnO_2/2Sb_2O_3$ fPVC film and the $2ZB/2Sb_2O_3$ fPVC film were reduced by 18.4 and 6.1°C, respectively, compared to that of $4Sb_2O_3$ fPVC film. These results indicated that the introduction of SnO_2 or ZB accelerated the early decomposition of the fPVC film.[37–39] Dogan et al.[38] found that ZB underwent thermal decomposition to produce H_2O (g), ZnO, and B_2O_3 at $T_{5\%}$. The H_2O (g) acted in the gas phase by leaving the char layer, while ZnO and B_2O_3 remained in the char layer to act in the condensed phase.[39] Moreover, the first maximum decomposition temperature (T_{max1}) of the $2SnO_2/2Sb_2O_3$ fPVC film decreased by 36.9°C, while that of the $2ZB/2Sb_2O_3$ fPVC film decreased by 66.8°C, in comparison to that of $4Sb_2O_3$ fPVC film. This decrease was mainly due to SnO_2 and ZnO captured a portion of the HCl during the initial de—HCl process,[27] resulting in the generation of $SnCl_2$ and $ZnCl_2$.[31,32] The compound acted as a catalyst in breaking down the fPVC film and promoting early cross-linking of the fPVC film,[24] leading to the formation of the char layer.[19] These results were consistent with those obtained from the SEM-EDS analysis.

Between 414 and 526°C, the mass loss primarily due to the degradation of molecular chains in the fPVC film.[50] The second maximum decomposition temperature (T_{max2}) of the $2SnO_2/2Sb_2O_3$ fPVC film and $2ZB/2Sb_2O_3$ fPVC film increased by 17.2°C and 14.3°C, respectively, compared to that of the $4Sb_2O_3$ fPVC film. This indicated that the partial replacement of Sb_2O_3 by SnO_2 or ZB can significantly improve the thermal stability of fPVC film,[27] which was mainly attributed to the fact that both SnO_2 and ZB can enhance the char formation ability of the materials.[19,38]

The residual at 600°C (R_{600}) of the $2SnO_2/2Sb_2O_3$ fPVC film and $2ZB/2Sb_2O_3$ fPVC film increased from 5.6 wt% to 11.9 wt% and 14.8 wt%, respectively, compared to that of $4Sb_2O_3$ fPVC film. This results indicated that the inclusion of SnO_2 or ZB improved the charring ability of fPVC film during thermal decomposition, which can effectively isolate the heat and oxygen resulting in better flame retardant properties for the fPVC film.[32] In conclusion, ZB exhibited a more effective catalytic charring effect than SnO_2.[28]

3.5 | Analysis of gas phase thermally decomposed products

To investigate the role of SnO_2/Sb_2O_3 and ZB/Sb_2O_3 in fPVC films and its flame retardant mechanism, TG-FTIR

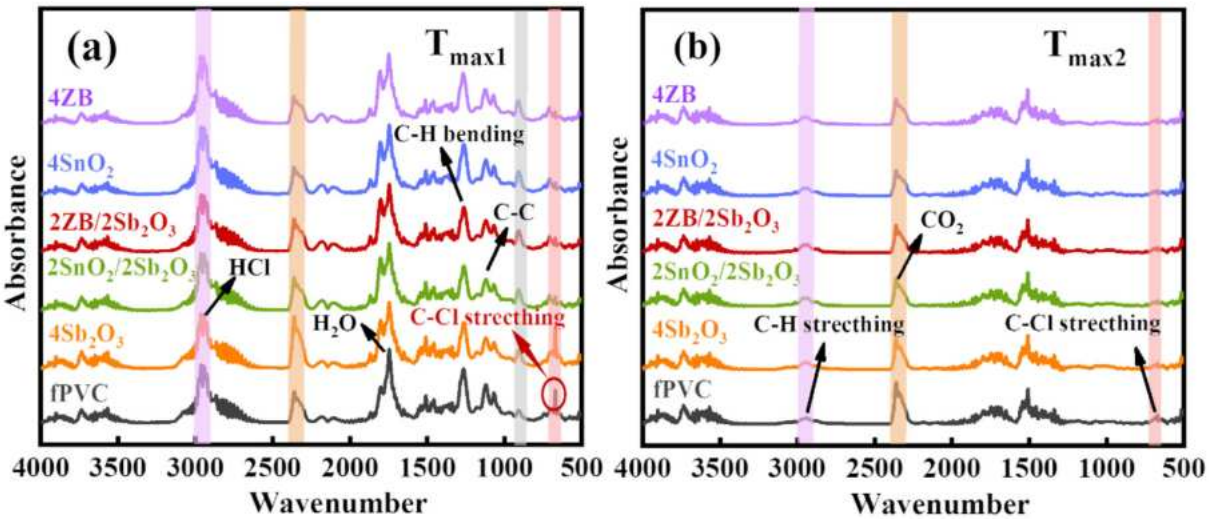

FIGURE 5 Infrared spectrum of thermal decomposition volatiles of flexible PVC (fPVC) films. ((a) T_{max1}, (b) T_{max2}). [Color figure can be viewed at wileyonlinelibrary.com]

was utilized to monitor the gas phase decomposition products of the fPVC film. Figure 5 showed the infrared spectrum of volatiles from thermal decomposition of the fPVC film, and Figure 5a,b represents the thermal decomposition volatiles spectra of the fPVC film at the first and second maximum decomposition temperature (T_{max1} and T_{max2}), respectively.

In Figure 5a, it can be observed that the C—Cl stretching peak (660 cm^{-1})[51,52] of the fPVC film was noticeably weakened, while the intensity of the HCl peak (3150–2500 cm^{-1})[53] was improved after replacing 50% Sb_2O_3 with SnO_2 or ZB. This was mainly due to the reaction of SnO_2 or ZnO (produced by thermal decomposition of ZB)[23] with HCl during thermal decomposition,[24] resulting in the formation of $SnCl_2$[31] or $ZnCl_2$.[9] These compounds catalyzed the de—HCl reaction of fPVC film and ultimately led to the breakage of more C—Cl bonds in the fPVC chains,[37] which ultimately led to a decrease in the intensity of the C—Cl stretching absorption peak and an increase of the intensity of the HCl absorption peak. In Figure 5b, the internal structural changes and hydrocarbon volatilization of the fPVC films during the second stage of thermal decomposition became insignificant, due to cross-linking and char formation caused by the flame retardant in the first stage.

Figure 6 showed the real-time tracking curves of the thermal decomposition volatiles of fPVC films. As shown in Figure 6a, the absorption intensities of C—Cl in the 2ZB/2Sb_2O_3 fPVC film were significantly lower than those in the 2SnO_2/2Sb_2O_3 fPVC film, while as shown in Figure 6b, the absorption intensities of HCl were significantly higher. The above results indicated that $ZnCl_2$ accelerated the initial decomposition of fPVC film and promoted the formation of a char layer more effectively than $SnCl_2$.[28] This led to the production of more HCl (g) in the gas phase and more char layer in the condensed phase.[38] Furthermore, as shown in Figure 6c,d, the absorption intensities of C—C (1120 cm^{-1}) and C—H bending (1266 cm^{-1})[51–53] in 2ZB/2Sb_2O_3 fPVC film were significantly lower than those in 2SnO_2/2Sb_2O_3 fPVC film. This indicated that ZB exhibited superior char-forming properties and barrier protection compared to SnO_2, which permitted the trapping of a greater quantity of char-containing and oxygen-containing components within the condensed phase.[39]

In conclusion, these processes not only reduced the oxygen concentration in the gas phase but also enhanced the barrier protection of the condensed phase, which played an important role in improving the flame retardancy and smoke suppression of fPVC film. The above results were consistent with those obtained from TGA and SEM-EDS.

3.6 | Flame retardant mechanism

Based on the results and discussions above, Figure 7 illustrated the flame retardant mechanism of SnO_2/Sb_2O_3 and ZB/Sb_2O_3 in fPVC films.

According to the previous discussion, Sb_2O_3 only exhibited a flame retardant effect in the gas phase. During the initial stage of combustion, Sb_2O_3 decomposed rapidly, and reacted with some of the HCl released from the fPVC film, producing $SbCl_3$ (g).[9] This $SbCl_3$ (g), which have a higher vapor density, covering the flame and isolating the oxygen.[32] Additionally, the remaining

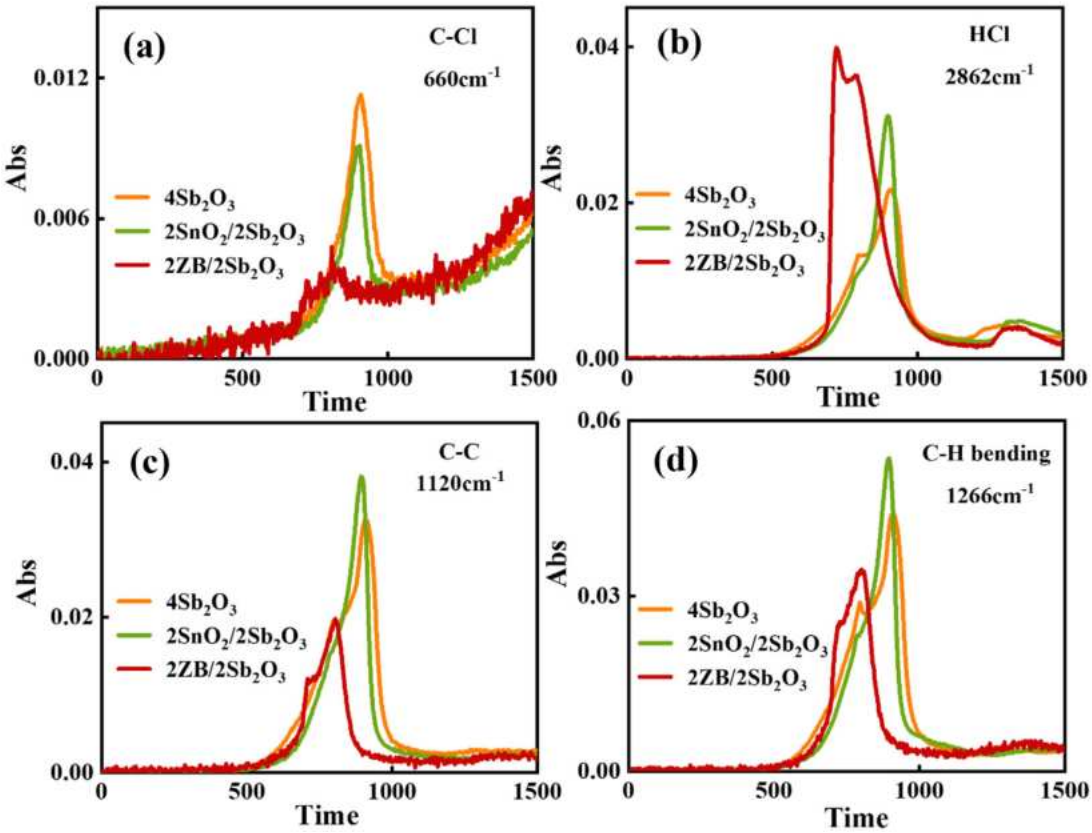

FIGURE 6 Real-time tracking curves of thermal decomposition volatiles of flexible PVC (fPVC) films ((a) C—Cl, (b) HCl, (c) C—C, (d) C—H bending). [Color figure can be viewed at wileyonlinelibrary.com]

HCl (g) was released into the gas phase, diluting the oxygen concentration.[19] Furthermore, it was worth noting that the decomposition of Sb_2O_3 was a heat-absorbing reaction that lowered the temperature in the vicinity of the flame.[49] While Sb_2O_3 was known for its excellent gas phase flame retardancy, it produced harmful gases and has a weak ability to char in the condensed phase. Therefore, it was important to replace some of the Sb_2O_3 with environmentally friendly flame retardants that have a strong charring ability.

The addition of either SnO_2 or ZB can compensate for the deficiency of Sb_2O_3 in the condensed phase charring formation ability. Furthermore, ZB exhibited superior charring ability, which enhanced the flame retardancy and smoke suppression of fPVC films. During combustion, SnO_2 reacted with some of the HCl released from fPVC to form $SnCl_2$, a strong Lewis acid.[31] These Lewis acid accelerated the detachment of HCl from the fPVC film,[19] generating more HCl (g) and promoting the cross-linking and charring of the fPVC film matrix.[37] This process produced more residual char within the condensed phase, resulting in a decrease in the concentration of oxygen in the gas phase and enhancing the barrier protection provided by the condensed phase.[27] Moreover, during the initial combustion phase, ZB decomposed into H_2O (g), ZnO, and B_2O_3. The H_2O (g) exited the char layer and was released into the gas phase,[38] which diluted the oxygen concentration and reduced the heat around the flame.[23] The ZnO and B_2O_3 were retained in the condensed phase, and the ZnO reacted with some of the HCl released from fPVC film to form $ZnCl_2$.[9] These $ZnCl_2$ enhanced the charring ability of fPVC film,[24] and their catalytic charring effect was superior to that of $SnCl_2$.[28] Furthermore, B_2O_3 accelerated the dehydration and charring of the fPVC film, resulting in a more stable char layer.[38] This layer acted as a barrier, reducing heat exchange, and trapping more fuels.[39] The flame retardant effects of ZB rendered it a superior alternative to Sb_2O_3, exhibiting more effective flame retardant and smoke suppression properties than SnO_2.

In conclusion, the addition of SnO_2 or ZB compensated for the deficiency of Sb_2O_3 in the condensed phase flame retardant effect, resulting in improved flame retardant properties for the fPVC films. Moreover, replacing 50% of Sb_2O_3 with ZB not only improved flame retardancy and smoke suppression, but also provided better cost-effective, health, and environmental protection than SnO_2. This made the ZB/Sb_2O_3 flame retardant system

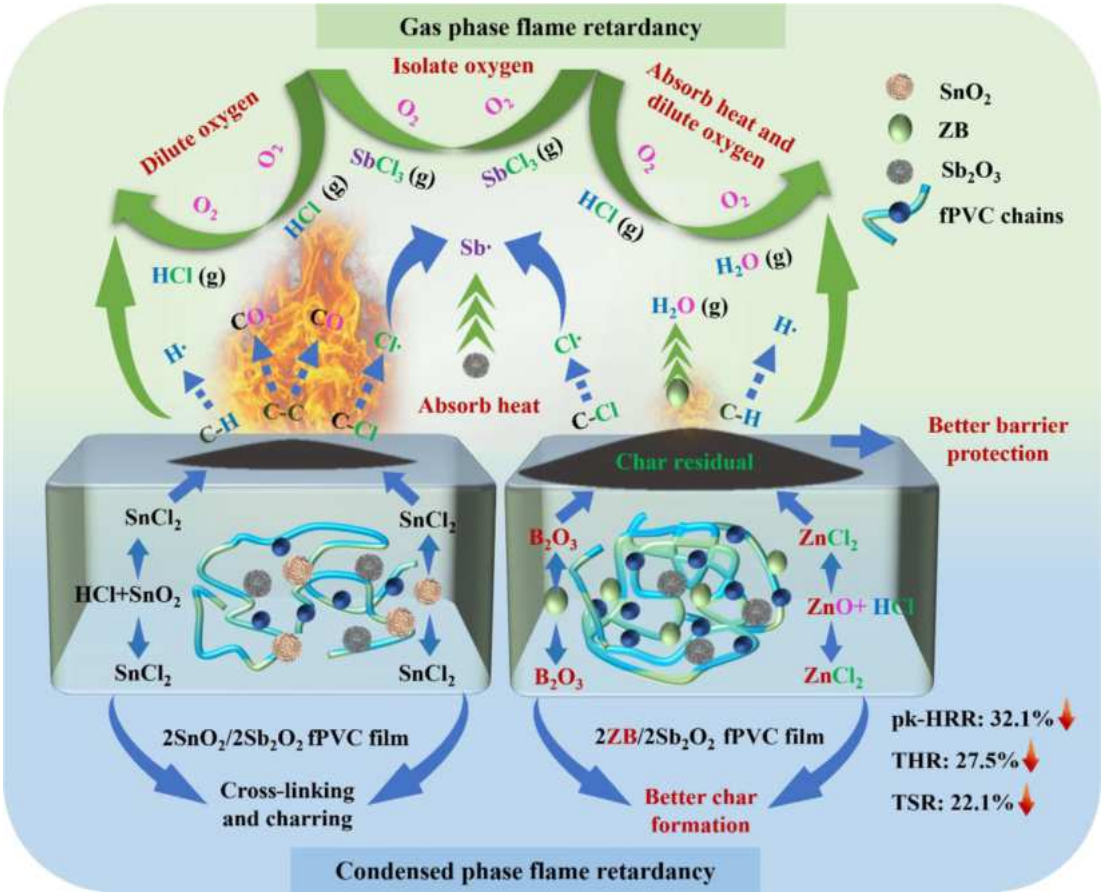

FIGURE 7 Flame retardant mechanism of flexible PVC (fPVC) films. [Color figure can be viewed at wileyonlinelibrary.com]

more suitable for the industrial application of the new generation of environmentally friendly automotive interior materials.

3.7 | Mechanical performance analysis

The mechanical properties of fPVC films were tested using a universal material testing machine to investigate the effects of SnO_2/Sb_2O_3 and ZB/Sb_2O_3 on their tensile strength and elongation at break. The results of the tensile test were presented in Table 5 The microscopic morphology of the fracture surfaces of the fPVC films were showed in Figure 8.

The pure fPVC film demonstrated excellent flexibility due to the addition of the plasticizer,[9] with an elongation at break of up to 190.6 ± 8.3%. The tensile strength and elongation at break of the fPVC film slightly increased with the addition of 4 phr Sb_2O_3.[31] Moreover, Figure 8b illustrated that SnO_2 displayed excellent dispersion and compatibility in fPVC films, resulting in materials with tensile strength (2.1 ± 0.07 MPa) and elongation at break (180.5 ± 13.0%) that were comparable to those of pure fPVC and $4Sb_2O_3$ fPVC films.

TABLE 5 Tensile test results of flexible PVC (fPVC) films.

Sample	Tensile strength (MPa)	Elongation at break (%)
fPVC	2.2 ± 0.04	190.6 ± 8.3
$4Sb_2O_3$	2.6 ± 0.02	194.8 ± 4.4
$1SnO_2/3Sb_2O_3$	2.1 ± 0.04	180.6 ± 5.4
$2SnO_2/2Sb_2O_3$	2.1 ± 0.07	180.5 ± 13.0
$3SnO_2/1Sb_2O_3$	2.1 ± 0.05	170.2 ± 6.3
$4SnO_2$	2.2 ± 0.06	173.6 ± 10.8
$1ZB/3Sb_2O_3$	2.1 ± 0.03	179.2 ± 7.2
$2ZB/2Sb_2O_3$	2.1 ± 0.04	174.8 ± 7.4
$3ZB/1Sb_2O_3$	2.5 ± 0.05	183.4 ± 8.4
4ZB	2.1 ± 0.04	177.9 ± 5.3

The $2ZB/2Sb_2O_3$ fPVC film exhibited a tensile strength of 2.1 ± 0.04 MPa and an elongation at break of 174.8 ± 7.4%. The observed reduction in elongation at break of the material in comparison to the $4Sb_2O_3$ and $2SnO_2/2Sb_2O_3$ fPVC films can be attributed primarily to the inadequate dispersion of ZB within the fPVC matrix. And the particle size of ZB was

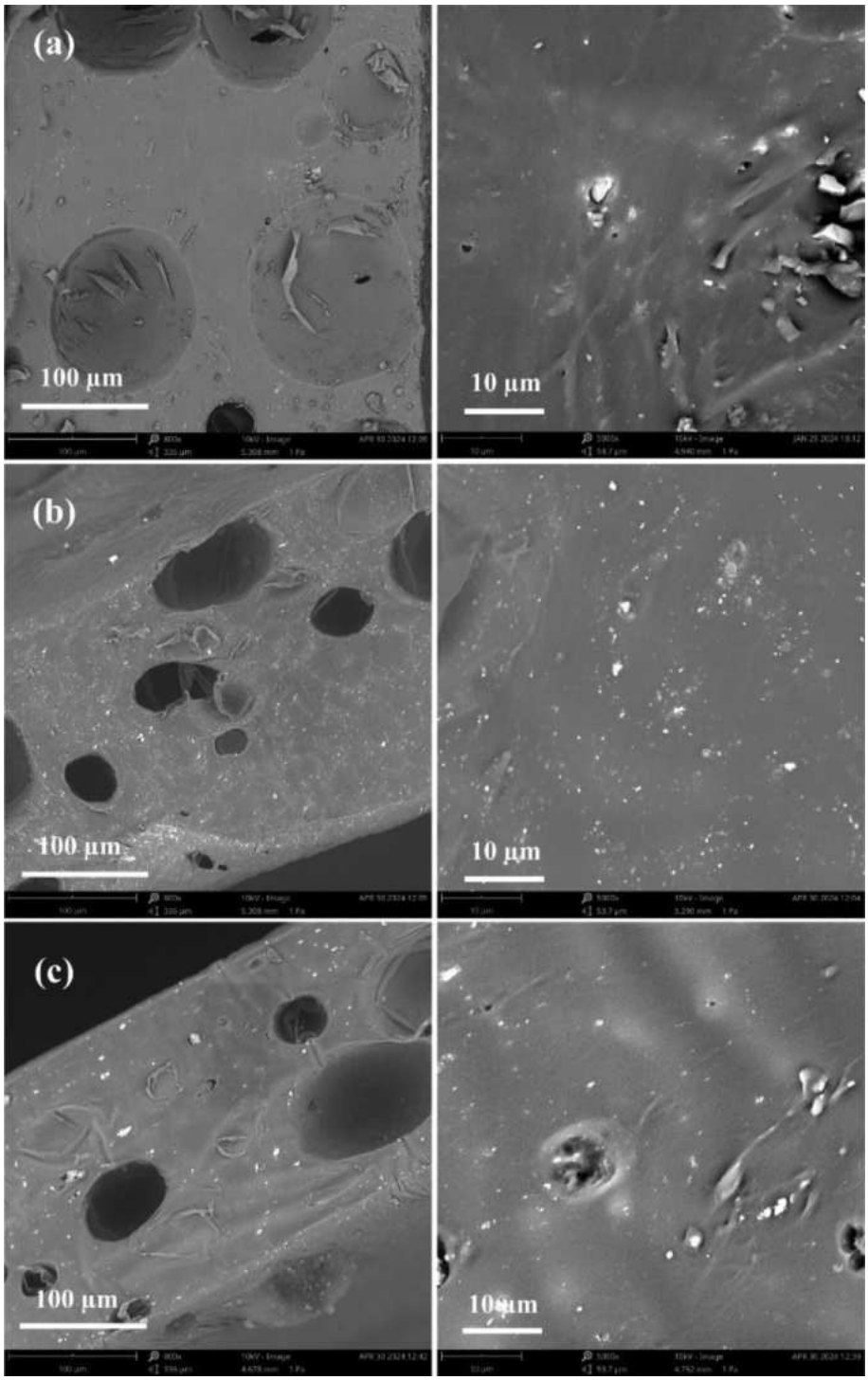

FIGURE 8 Microscopic morphology of the fracture surfaces of the flexible PVC (fPVC) films. ((a) $4Sb_2O_3$, (b) $2SnO_2/2Sb_2O_3$, (c) $2ZB/2Sb_2O_3$).

considerably larger than that of SnO_2 and Sb_2O_3, which resulted in a reduced compatibility between ZB and fPVC matrix. However, in the production of automotive interior materials, fPVC films were typically adhered to a base cloth that exhibited considerable flexibility.[47] Accordingly, a reduction in the elongation at break of fPVC films did not directly impact the practical application of the material in the automotive interior industry.

In conclusion, these results indicated that the replacement of 50% of Sb_2O_3 with SnO_2 or ZB did not compromise the suitability of fPVC films for industrial applications in automotive interior materials.[32]

4 | CONCLUSION

In this work, two environmentally friendly flame retardants, SnO_2 and ZB, were used as partial replacement for Sb_2O_3. Both significantly improved the flame retardancy of fPVC film, but ZB showed superior flame retardancy and

smoke suppression. Compared to the $4Sb_2O_3$ fPVC film, the $2ZB/2Sb_2O_3$ fPVC film demonstrated superior ignition resistance and self-extinguishing properties. Additionally, the material exhibited a 32.1% reduction in PHRR, a 27.5% reduction in THR, and a 22.1% reduction in TSR, compared to that of the $4Sb_2O_3$ fPVC film. The improved flame retardancy of fPVC film was attributed to the presence of ZB, which compensated for the deficiency flame retardancy of Sb_2O_3 in the condensed phase. During the initial combustion stage, ZB decomposed into H_2O (g), ZnO, and B_2O_3, which exhibited flame retardant paths at different levels. Therefore, ZB/Sb_2O_3 system was more suitable for industrial applications in automotive interior materials. The development of this new flame retardant system provided valuable insights for the production and use of fPVC films. These fPVC film are expected to become a new generation of environmentally friendly automotive interior materials.

AUTHOR CONTRIBUTIONS

Lijun Qian: Conceptualization (lead); supervision (lead); writing – review and editing (lead). **Yongsen Zhang:** Data curation (lead); investigation (lead); methodology (lead); writing – original draft (lead). **Lijie Qu:** Funding acquisition (lead); writing – review and editing (lead). **Jingyu Wang:** Data curation (supporting); funding acquisition (supporting); writing – review and editing (supporting). **Yong Qiu:** Writing – review and editing (supporting). **Wang Xi:** Writing – review and editing (supporting). **Yao Ma:** Conceptualization (supporting); funding acquisition (supporting).

ACKNOWLEDGMENTS

This work was supported by National Natural Science Foundation of China (nos. 12302272, 22005009, 52203055), Beijing Natural Science Foundation (no. 2222052), and R&D Program of Beijing Municipal Education Commission (KM202210011004).

CONFLICT OF INTEREST STATEMENT

The authors declare that they have no known competing financial interests or personal relationships that could have appeared to influence the work reported in this paper.

DATA AVAILABILITY STATEMENT

Data will be made available on request.

ORCID

Lijun Qian https://orcid.org/0000-0002-8847-4934

REFERENCES

[1] P. Gupta, B. Toksha, B. Patel, Y. Rushiya, P. Das, M. Rahaman, *Chem. Rec.* **2022**, *22*, e202200186.
[2] Z. H. Wu, A. C. Huang, Y. Tang, Y. P. Yang, Y. C. Liu, Z. P. Li, H. L. Zhou, C. F. Huang, Z. X. Xing, C. M. Shu, J. C. Jiang, *Polymer* **2021**, *13*, 1675.
[3] G. Zattini, S. Ballardini, T. Benelli, L. Mazzocchetti, L. Giorgini, *Polym. Eng. Sci.* **2019**, *59*, 2488.
[4] X. B. Ma, H. Yun, N. J. Wu, F. K. Niu, J. H. Yu, A. C. S. Appl, *Polym. Mater.* **2021**, *3*, 1314.
[5] V. Najafi, H. Abdollahi, *Eur. Polym. J.* **2020**, *128*, 109620.
[6] W. An, J. Z. Ma, Q. N. Xu, H. Zhang, *Compos. Pt. A-Appl. Sci. Manuf.* **2023**, *165*, 107327.
[7] Y. C. Li, L. D. Lv, W. S. Wang, J. X. Zhang, J. Lin, J. Y. Zhou, M. Y. Dong, Y. F. Gan, I. Seok, Z. H. Guo, *Polymer* **2020**, *190*, 122198.
[8] S. H. Lee, G. R. Yi, D. Y. Lim, W. Y. Jeong, J. H. Youk, *Fiber. Polym.* **2019**, *20*, 779.
[9] L. Zhang, T. T. Chen, J. Zhang, *J. Appl. Polym. Sci.* **2023**, *141*, e54790.
[10] B. F. Qian, W. Y. Wang, H. C. Zhu, J. N. Zhang, M. Y. Wu, J. Y. Liu, Q. Y. Wu, J. J. Yang, *Chem. Eng. J.* **2023**, *476*, 146859.
[11] C. H. Gao, Y. Q. Wang, Y. L. Gao, R. X. Wang, H. Z. Wang, Y. M. Wu, Y. T. Liu, *J. Polym. Environ.* **2022**, *30*, 4651.
[12] Y. J. Ma, X. G. Dang, Z. H. Shan, *J. Therm. Sci.* **2019**, *28*, 88.
[13] M. Gao, M. Wan, X. Zhou, *J. Therm. Anal. Calorim.* **2019**, *138*, 387.
[14] Q. Y. Xie, T. Gong, X. Y. Huang, *Fire. Technol.* **2021**, *57*, 2643.
[15] Z. Y. Huo, H. J. Wu, Q. Y. Song, Z. X. Zhou, T. Wang, J. X. Xie, H. Q. Qu, *Carbohydr. Polym.* **2021**, *256*, 117575.
[16] P. Xiang, J. Xu, B. Li, W. Q. Liu, J. S. Zhao, Q. N. Ke, S. W. Bi, X. H. Chen, *Dent. Mater.* **2021**, *14*, 2634.
[17] W. D. Hu, J. Wu, Y. H. Jiao, J. X. Xie, J. J. Chen, J. Z. Xu, *J. Fire Sci.* **2018**, *37*, 67.
[18] W. H. Meng, Y. L. Dong, J. H. Li, L. Y. Cheng, H. J. Zhang, C. Z. Wang, Y. H. Jiao, J. Z. Xu, J. W. Hao, H. Q. Qu, *Compos. Pt. B-Eng.* **2020**, *188*, 107854.
[19] Y. T. Pan, M. Castillo-Rodríguez, D. Y. Wang, *Mater. Chem. Phys.* **2018**, *203*, 49.
[20] H. L. Shi, Z. W. Li, X. H. Li, Z. J. Zhang, *J. Appl. Polym. Sci.* **2022**, *139*, e52210.
[21] W. H. Meng, W. H. Wu, W. W. Zhang, L. Y. Cheng, Y. H. Jiao, H. Q. Qu, J. Z. Xu, *Micro Nano Lett.* **2019**, *14*, 828.
[22] X. Q. Qiu, D. Q. Wang, Q. Li, X. Y. Li, X. W. Zhao, Z. W. Li, X. H. Li, Z. J. Zhang, *J. Appl. Polym. Sci.* **2022**, *139*, e51724.
[23] W. J. Diao, Z. J. Liu, G. M. Yuan, E. X. Jiao, K. X. Wang, H. Yang, Z. Li, K. Wu, J. Shi, *Polym. Degrad. Stab.* **2023**, *214*, 110404.
[24] Y. Xu, R. Zhou, J. J. Mu, Y. M. Ding, J. C. Jiang, *Colloid Surf. A-Physicochem. Eng. Asp.* **2022**, *640*, 128400.
[25] Y. Seki, M. M. Tokgöz, F. Öner, M. Sarikanat, L. Altay, *ACS Omega* **2023**, *8*, 19265.
[26] E. M. Alosime, A. A. Basfar, *Molecules* **2023**, *28*, 1023.
[27] Y. T. Pan, Y. S. Yuan, D. Y. Wang, R. J. Yang, *Chin. J. Chem.* **2022**, *38*, 1870.
[28] Y. Q. Fang, A. J. Xue, F. Q. Wang, Z. J. Zhang, Y. M. Song, W. H. Wang, Q. Wang, *Constr. Build. Mater.* **2022**, *320*, 126203.
[29] Y. Y. Chan, C. Ma, F. Zhou, Y. Hu, B. Schartel, *Polym. Adv. Technol.* **2021**, *33*, 326.
[30] Y. Qiu, B. A. Xi, L. J. Qian, A. Q. Liu, L. B. Gao, *Polym. Adv. Technol.* **2022**, *33*, 3238.

[31] Y. T. Pan, M. Castillo-Rodríguez, D. Y. Wang, *Chem. Eng. J.* **2016**, *295*, 451.
[32] Y. N. Chen, Q. S. Wu, N. Li, T. Tang, X. Xie, C. C. Zhang, Y. X. Zuo, *CoatingsTech* **2023**, *13*, 1814.
[33] W. Tang, L. J. Qian, Y. J. Chen, Y. Qiu, B. Xu, *Polym. Degrad. Stab.* **2019**, *169*, 108982.
[34] J. X. Li, L. J. Qian, W. Xi, Y. Qiu, W. Tang, S. Z. Li, *J. Appl. Polym. Sci.* **2022**, *139*, e53226.
[35] X. Wu, L. J. Qian, W. Xi, Y. Qiu, J. Li, *Eur. Polym. J.* **2023**, *196*, 112289.
[36] L. J. Qian, L. J. Li, Y. J. Chen, B. Xu, Y. Qiu, *Compos. Pt. B-Eng.* **2019**, *175*, 107186.
[37] L. Dang, Z. H. Lv, X. Liu, *J. Appl. Polym. Sci.* **2021**, *138*, e51061.
[38] M. Dogan, S. D. Dogan, L. A. Savas, G. Ozcelik, U. Tayfun, *Compos. Pt. B-Eng.* **2021**, *222*, 109088.
[39] Y. T. Pan, X. Wang, Z. Li, D. Y. Wang, *Compos. Pt. B-Eng.* **2017**, *110*, 46.
[40] W. Tang, L. J. Qian, S. G. Prolongo, D. Y. Wang, *Chem. Eng. J.* **2023**, *471*, 144716.
[41] J. Feng, J. W. Hao, J. X. Du, R. J. Yang, *Polym. Degrad. Stab.* **2012**, *97*, 605.
[42] K. Salasinska, K. Mizera, M. Celinski, P. Kozikowski, J. Mirowski, A. Gajek, *Fire Saf. J.* **2021**, *122*, 103326.
[43] T. T. Gao, Z. W. Li, L. G. Yu, Z. J. Zhang, *RSC Adv.* **2015**, *5*, 99291.
[44] T. T. Gao, L. C. Chen, Z. W. Li, L. G. Yu, Z. S. Wu, Z. J. Zhang, *Nanoscale Res. Lett.* **2016**, *11*, 192.
[45] B. Sang, Z. W. Li, L. G. Yu, X. H. Li, Z. J. Zhang, *Mater. Lett.* **2017**, *204*, 133.
[46] J. S. Xu, H. Y. Yang, Z. B. Luo, D. Wu, G. Y. Cao, *RSC Adv.* **2022**, *12*, 2914.
[47] Y. S. Zhang, L. J. Qian, L. J. Qu, J. Y. Wang, Y. Qiu, W. Xi, Y. Ma, *React. Funct. Polym.* **2024**, *197*, 105864.
[48] H. Q. Qu, W. H. Wu, Y. J. Zheng, J. X. Xie, J. Z. Xu, *Fire Saf. J.* **2011**, *46*, 462.
[49] J. X. Wang, X. Zhao, Q. Yu, S. Zhang, *Thermochim. Acta* **2021**, *700*, 178935.
[50] M. L. Xu, C. Y. Cao, H. Y. Hu, Y. Ren, G. Z. Guo, L. F. Gong, J. W. Zhang, T. Zhang, H. Yao, *Fuel* **2022**, *327*, 125082.
[51] J. Yu, L. S. Sun, C. Ma, Y. Qiao, H. Yao, *Waste Manag.* **2016**, *48*, 300.
[52] L. Dang, Z. H. Lv, X. L. Du, D. L. Tang, Y. T. Zhao, D. H. Zhu, S. A. Xu, *Polym. Adv. Technol.* **2020**, *31*, 2108.
[53] Y. L. Wang, N. Kang, J. Lin, S. X. Lu, K. M. Liew, *J. Anal. Appl. Pyrolysis* **2023**, *170*, 105901.

SUPPORTING INFORMATION

Additional supporting information can be found online in the Supporting Information section at the end of this article.

How to cite this article: Y. Zhang, L. Qian, L. Qu, J. Wang, Y. Qiu, W. Xi, Y. Ma, *J. Appl. Polym. Sci.* **2024**, *141*(40), e56045. https://doi.org/10.1002/app.56045